ACS APPLIED MATERIALS & INTERFACES

Letter

Cite This: ACS Appl. Mater. Interfaces 2018, 10, 43299−43304

www.acsami.org

Synthesis of Two-Dimensional Alloy $Ga_{0.84}In_{0.16}Se$ Nanosheets for High-Performance Photodetector

Miaomiao Yu,[†,‡] Hang Li,[†,§] He Liu,[‡] Fanglu Qin,[‡] Feng Gao,[⊥] Yunxia Hu,[⊥] Mingjin Dai,[⊥] Lifeng Wang,[∥] Wei Feng,[*,‡] and PingAn Hu[*,⊥]

[‡]Department of Chemistry and Chemical Engineering, College of Science, Northeast Forestry University, Harbin, 150040, China

[§]Innovation Lab of Space Robot System, Space Robotics Engineering Center, Changchun Institute of Optics, Fine Mechanics and Physics, Chinese Academy of Sciences, Changchun 130033, China

[⊥]Key Lab of Microsystem and Microstructure of Ministry of Education, Harbin Institute of Technology, Harbin 150080, China

[∥]Institute for Frontier Materials, Deakin University, 75 Pigdons Road, Waurn Ponds, Geelong, Victoria 3216, Australia

Supporting Information

Downloaded via CHANGCHUN INST OMP on August 15, 2019 at 08:26:46 (UTC).
See https://pubs.acs.org/sharingguidelines for options on how to legitimately share published articles.

ABSTRACT: The electronic and optoelectronic properties of 2D alloy $Ga_{0.84}In_{0.16}Se$ were investigated for the first time. 2D $Ga_{0.84}In_{0.16}Se$ FETs show p-type conduction behaviors. 2D $Ga_{0.84}In_{0.16}Se$ photodetectors show high photoresponse in the visible light range of 500 to 700 nm. The responsivity value is 258 A/W for alloy photodetector (500 nm illumination), and it is 92 times and 20 times higher than those of 2D GaSe and InSe photodetectors, respectively. Moreover, the alloy photodetector exhibits good photoresponse stability and rapid photoresponse time. Our results demonstrate that 2D alloy $Ga_{0.84}In_{0.16}Se$ has great potential for application in photodetection and sensor devices.

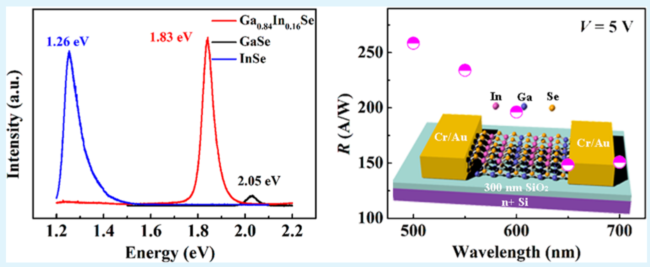

KEYWORDS: *$Ga_{0.84}In_{1.86}Se$, alloy engineering, photodetectors, two-dimensional materials, III−VI group semiconductors*

The discovery of graphene paved the way for the research on two-dimensional (2D) materials.[1] To date, many 2D materials have been explored, such as semimetallic graphene,[1] insulating h-BN,[2] semiconducting transition-metal dichalcogenides (TMDs[3]), black phosphorus,[4] IV−VI group compounds[5−7] and III−VI group compounds (GaSe,[8−10] GaTe[11] and InSe,[12−14] etc.). Compared to 0D and 1D materials,[15,16] 2D semiconductors are more compatible with modern semiconducting fabrication technology. 2D semiconductors show great potential for application in new generation of electronic and optoelectronic devices.[17−20] Among the large family of 2D semiconductors, 2D layered III−VI group semiconductors (such as GaSe and InSe) have received sustained attention because of their novel electrical and optical properties. Photodetectors composed of 2D GaSe show a high photoresponsivity.[8,9] 2D GaSe is a good nonlinear optical semiconductor[16] and shows a strong optical second-harmonic generation (SHG) signal, which is much larger than that of monolayer MoS_2.[21] These properties demonstrate that 2D GaSe can be applied in future nanophotonic devices. Additionally, 2D InSe shows outstanding and stable electronic and optoelectronic properties, such as a high electron mobility of 1×10^4 cm^2 V^{-1} s^{-1} at low temperature and high photoresponsivity under a broad spectral response range from ultraviolet (UV) to near-infrared (NIR) light.[13,14] Multilayer InSe has a direct bandgap of 1.26 eV, which is independent of its thickness (>20 nm). 2D InSe shows a better stability than black phosphorus in atmosphere.[14] These advantages indicate that 2D InSe has great potential for application in high-performance electronic and optoelectronic devices, such as FETs[12] and photodetectors.[13]

For expanding the applications of semiconductors, alloy engineering is an important and versatile strategy in bandgap engineering and tuning the electronic properties of bulk semiconductors. 0D and 1D ternary semiconductors show tunable bandgaps and light emissions by using different chemical constituents.[22,23] For 2D semiconductors, alloy engineering is mainly applied to 2D TMDs systems.[24−27] For example, alloy engineering successfully tunes not only the bandgap but also the charge carrier types in 2D $WS_{2x}Se_{2-2x}$.[25] However, 2D III−VI group alloy semiconductors are limited. In view of the merits of 2D GaSe and InSe, it is important to investigate the electronic and optoelectronic properties of $Ga_{1-x}In_xSe$ alloy.

In this letter, for the first time, we investigate the electronic and optoelectronic properties of 2D $Ga_{1-x}In_xSe$ (x = 0.16) alloy nanosheets. Bulk $Ga_{0.84}In_{0.16}Se$ alloy samples were synthesized and showed a direct optical bandgap of 1.83 eV. The 2D $Ga_{0.84}In_{0.16}Se$ nanosheets were obtained by mechanical exfoliation methods. The 2D $Ga_{0.84}In_{0.16}Se$ FETs showed p-

Received: September 4, 2018
Accepted: December 3, 2018
Published: December 3, 2018

 © 2018 American Chemical Society

DOI: 10.1021/acsami.8b15317
ACS Appl. Mater. Interfaces 2018, 10, 43299−43304

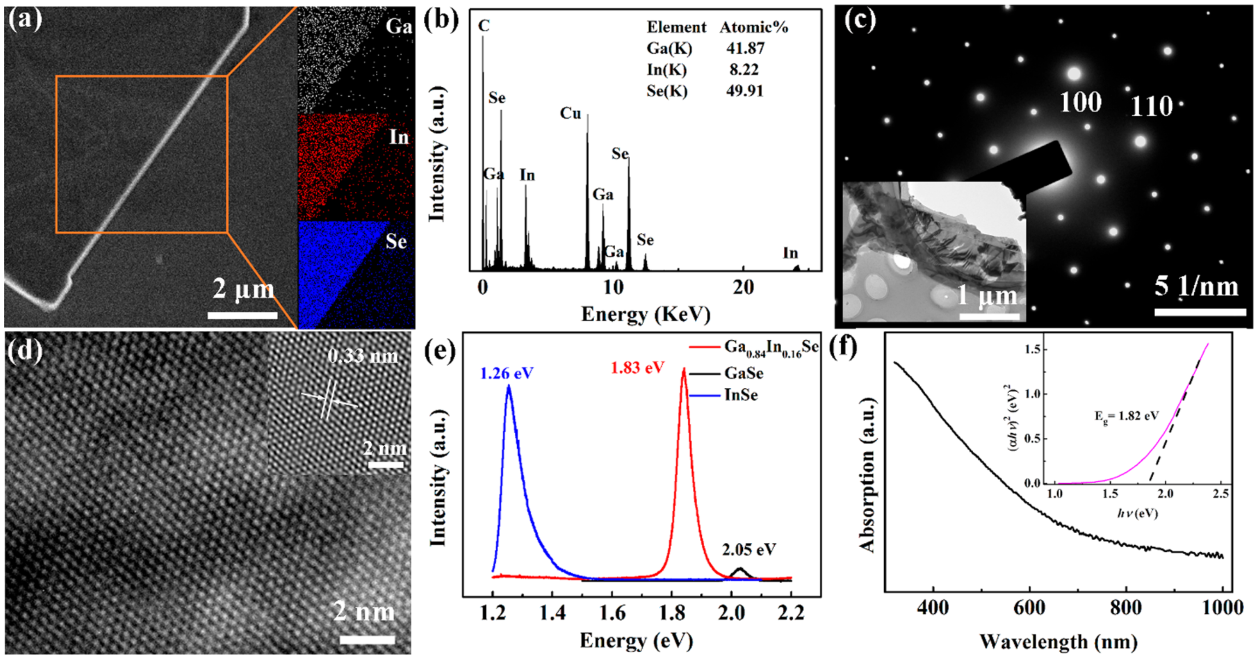

Figure 1. Structure characterizations of $Ga_{1-x}In_xSe$ (x = 0.16): (a) Elemental mapping image. (b) EDS image. (c) SAED pattern of $Ga_{0.84}In_{0.16}Se$. Inset: TEM image at low magnification. (d) HRTEM image of $Ga_{0.84}In_{0.16}Se$. Inset: the corresponding reverse Fourier transform pattern. (e) Photoluminescence (PL) spectra of $Ga_{0.84}In_{0.16}Se$, GaSe and InSe. (f) UV−vis−NIR absorption spectrum of the $Ga_{0.84}In_{0.16}Se$ alloy. Inset: the corresponding Tauc plot.

type conduction behaviors with a slightly higher mobility (0.8 $cm^2\ V^{-1}\ s^{-1}$) and current on/off ratio (1×10^5) than those of 2D GaSe FETs. The 2D $Ga_{0.84}In_{0.16}Se$ photodetectors showed a high photoresponse over a broad visible-light range (500−700 nm). The responsivity value is 258 A/W for the alloy photodetector, which is 92 times and 20 times higher than those of 2D GaSe and InSe photodetectors, respectively. Photodetectors based on 2D $Ga_{0.84}In_{0.16}Se$ also exhibited good photoresponse stability and rapid photoresponse time. Our results demonstrate that the 2D $Ga_{0.84}In_{0.16}Se$ alloy has great potential to be applied in photodetection and sensor devices.

Figure 1a is an SEM image and elemental mapping of a multilayer nanosheet on 300 nm SiO_2/Si substrate, which demonstrates that Ga, In and Se in the synthesized samples are homogeneously distributed over the selected area. To determine the chemical composition ratio in detail, we collected an X-ray energy-dispersive spectrum (EDS) (Figure 1b). The chemical composition ratio of Ga to In is 41.87:8.22 (0.84:0.16) and demonstrates that the synthesized sample is a $Ga_{1-x}In_xSe$ (x = 0.16) alloy, which coincides with eutectic gallium−indium. The chemical composition ratio of Ga/In to Se is approximately equal to 1:1, indicating that the structure of the synthesized $Ga_{0.84}In_{0.16}Se$ may be similar to that of GaSe. The chemical composition of the $Ga_{0.84}In_{0.16}Se$ sample was further examined by XPS (Figure S1). The peaks in the XPS spectrum are consistent with the Ga−Se and In−Se bonding features reported in an early study,[28] indicating successful In-doping. The atomic ratio of In, Ga and Se is consistent with EDS results. The crystal structure of $Ga_{0.84}In_{0.16}Se$ was examined by XRD (Figure S2). The main peaks are indexed to the hexagonal structure of GaSe, and the other small peaks are indexed to hexagonal structure of InSe, further indicating the successful In-doping. The XRD patterns demonstrate that the $Ga_{0.84}In_{0.16}Se$ alloy is highly c-axis oriented. The crystal microstructure of the $Ga_{0.84}In_{0.16}Se$ alloy was further examined by TEM analysis. A clean surface and layered structure are seen in the low magnification TEM image (Figure 1c inset). The selected area electron diffraction pattern (SAED) shows a set of diffraction spots (Figure 1c) and indicates that the synthesized $Ga_{0.84}In_{0.16}Se$ alloy possesses good crystallinity. The HRTEM image shows the perfect crystallinity of the $Ga_{0.84}In_{0.16}Se$ alloy with a lattice spacing of 3.3 Å in Figure 1d, which is slightly larger than 0.32 nm of GaSe[29] and smaller than 0.34 nm of InSe.[12] Figure S3 is the Raman spectrum of the $Ga_{0.84}In_{0.16}Se$ alloy. Most of Raman peaks belong to GaSe, and the peak at 188 cm^{-1} is indexed to the E^2 mode of In−Se bond, indicating the successful substitution of Ga atoms by In atoms. Figure 1e shows the PL reuslts of GaSe, InSe and the synthesized $Ga_{0.84}In_{0.16}Se$ alloy. The synthesized $Ga_{0.84}In_{0.16}Se$ alloy shows a strong PL peak at 1.83 eV and is completely different from the weak peak (2.05 eV) of GaSe that has an indirect optical bandgap, indicating the synthesized $Ga_{0.84}In_{0.16}Se$ alloy has a direct optical bandgap. To further quantitatively extract its bandgap, the optical absorption of the $Ga_{0.84}In_{0.16}Se$ alloy was measured, and the corresponding Tauc plot is shown in Figure 1f. The $Ga_{0.84}In_{0.16}Se$ alloy shows a broadband optical absorption ranging from UV to visible light regions, suggesting its great potential application in photodetection. The optical bandgap is extracted to be 1.82 eV from the Tauc plot, which is consistent with the PL result (see more detailed discussion in the Supporting Information). TGA was used to investigate the chemical and physical stability with respect to temperature. As shown in Figure S4, the $Ga_{0.84}In_{0.16}Se$ alloy owns a high thermal stability up to 873 K.

After successfully synthesizing the $Ga_{0.84}In_{0.16}Se$ alloy with good crystallinity, we investigated the electronic and optoelectronic properties of the 2D $Ga_{0.84}In_{0.16}Se$ alloy. Here, back-gated FETs and photodetectors of the 2D $Ga_{0.84}In_{0.16}Se$ alloy were fabricated. Both the electronic and optoelectronic properties of the 2D $Ga_{0.84}In_{0.16}Se$ devices were measured

DOI: 10.1021/acsami.8b15317
ACS Appl. Mater. Interfaces 2018, 10, 43299−43304

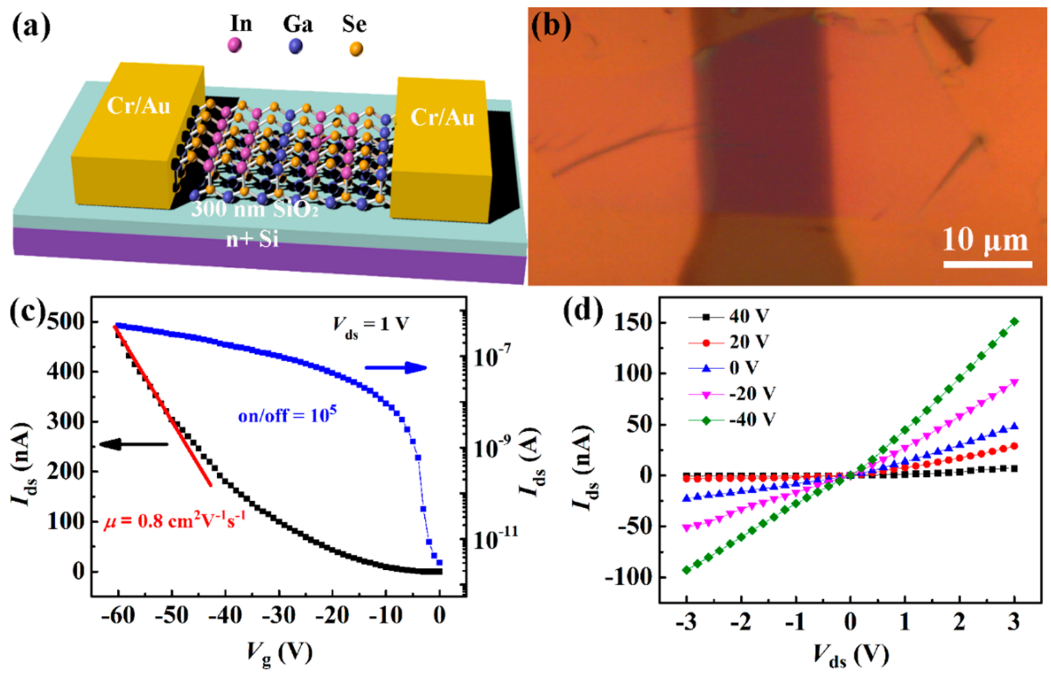

Figure 2. Structural and electronic characterization of 2D $Ga_{0.84}In_{0.16}Se$ FETs: (a) 3D schematic structure of $Ga_{0.84}In_{0.16}Se$ FETs. (b) A typical optical image of 2D $Ga_{0.84}In_{0.16}Se$ FETs. (c) Transfer curves of 2D $Ga_{0.84}In_{0.16}Se$ FETs measured at V_{ds} = 1 V. (d) Output curves of 2D $Ga_{0.84}In_{0.16}Se$ FETs measured at various gate voltages.

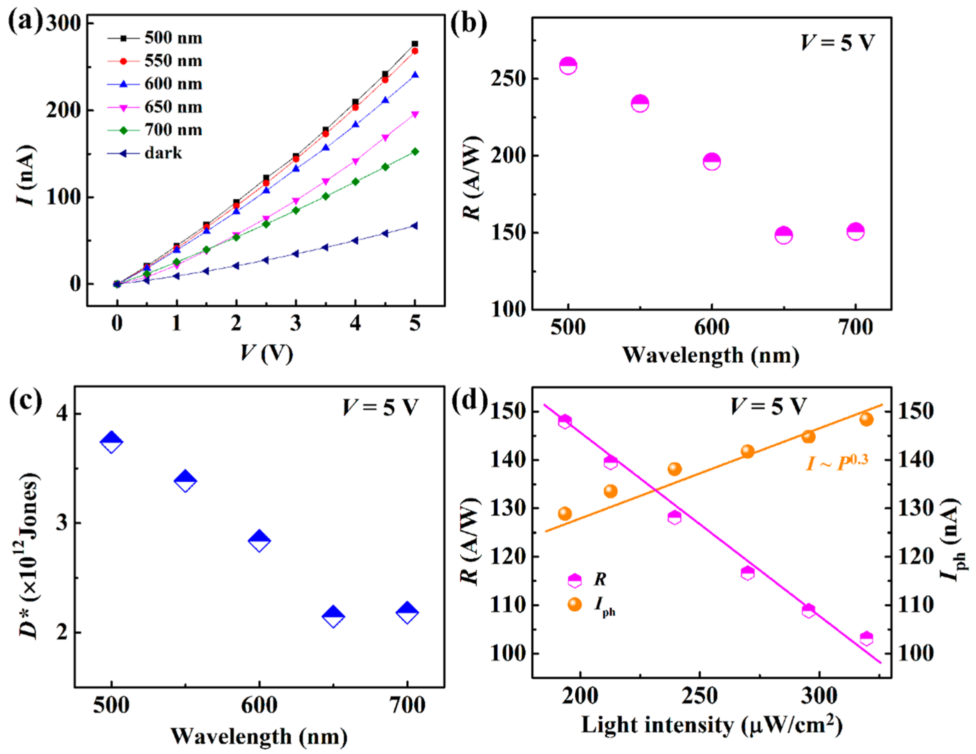

Figure 3. Photoresponse of the 2D $Ga_{0.84}In_{0.16}Se$ alloy. (a) $I-V$ curves of the 2D $Ga_{0.84}In_{0.16}Se$ alloy photodetector illuminated at different wavelengths. The illumination intensities are 180.9, 191.1, 196.2, 193.6, and 126.1 $\mu W/cm^2$ for 500, 550, 600, 650, and 700 nm, respectively. (b) R values and (c) D^* values for various wavelengths at V = 5 V. (d) I_{ph} and R values illuminated at 650 nm and V = 5 V with various light intensities.

under ambient conditions. As shown in Figure 2a, a few-layer $Ga_{0.84}In_{0.16}Se$ nanosheet is the channel material, Cr/Au electrodes work as source-drain electrodes, n-doped silicon is the gate and 300 nm silica works as the dielectric layer. Figure 2b is a typical optical image of the 2D $Ga_{0.84}In_{0.16}Se$ alloy FETs (channel length: 15 μm, channel width: 30 μm). Figure S5 shows the AFM results of 2D $Ga_{0.84}In_{0.16}Se$ alloy channel, which is 8 nm. Figure 2c shows the transfer curves of 2D $Ga_{0.84}In_{0.16}Se$ FETs, demonstrating that the 2D $Ga_{0.84}In_{0.16}Se$ alloy is a p-type semiconductor. The 2D $Ga_{0.84}In_{0.16}Se$ FETs show a current on/off ratio of 1×10^5, which is comparable to that of 2D GaSe FETs[8] and meets the requirement for

DOI: 10.1021/acsami.8b15317
ACS Appl. Mater. Interfaces 2018, 10, 43299−43304

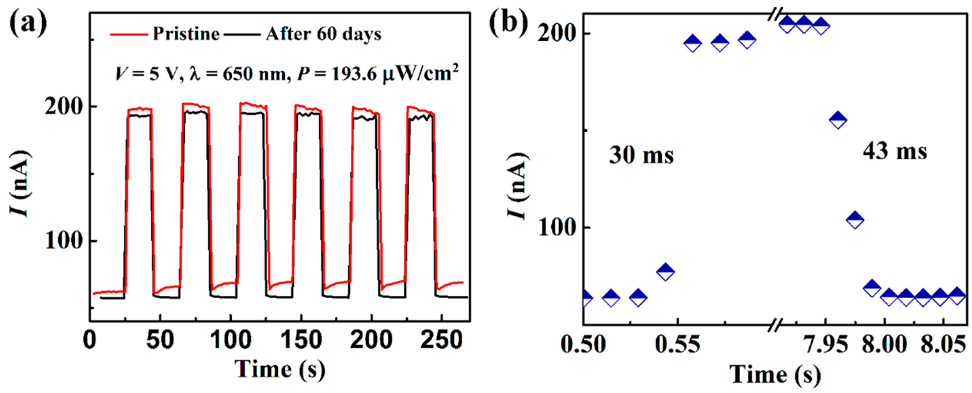

Figure 4. Stability and response time of $Ga_{0.84}In_{0.16}Se$ photodetectors. (a) Time-dependent photoresponse stability of $Ga_{0.84}In_{0.16}Se$ photodetectors illuminated at 650 nm light on day 0 and after storage in air for 60 days at V = 5 V with an illumination intensity of 193.6 $\mu W/cm^2$. (b) Corresponding response time.

practical application in COMS-like digital circuits. The field-effect mobility (μ) is 0.8 $cm^2\ V^{-1}\ s^{-1}$ for 2D $Ga_{0.84}In_{0.16}Se$ FETs, which is slightly higher than that of 2D GaSe FETs (see the Supporting Information for more detail).[8] Figure 2d shows the corresponding output curves of 2D $Ga_{0.84}In_{0.16}Se$ FETs measured at various gate voltages. The $I_{ds}-V_{ds}$ curves show good linear behavior, which is similar to 2D GaSe FETs.[8] The output curves further demonstrate that the synthesized $Ga_{0.84}In_{0.16}Se$ alloy is a p-type semiconductor because the output current decreases as the back-gate values increases. The contact resistance (R_c) between the $Ga_{0.84}In_{0.16}Se$ alloy and Cr metal electrode is roughly calculated to be 19 MΩ (more detailed discussion is in the Supporting Information). The contact resistance can be further reduced by optimizing the metal electrode.

To explore photoresponse properties of 2D $Ga_{0.84}In_{0.16}Se$ alloy, we used various illumination wavelengths ranging from 500 to 700 nm (wavelength increasing by a step of 50 nm) to vertically illuminate the 2D $Ga_{0.84}In_{0.16}Se$ photodetectors. The 2D $Ga_{0.84}In_{0.16}Se$ photodetectors show a wide visible-light range photoresponse from 500 to 700 nm as shown in Figure 3a. The response range of 2D $Ga_{0.84}In_{0.16}Se$ is slightly larger than that of 2D GaSe[9] (<700 nm), which is attributed to the smaller optical bandgap of $Ga_{0.84}In_{0.16}Se$ of 1.83 eV than that of GaSe. Responsivity (R), detectivity (D^*), and external quantum efficiency (EQE) are three key parameters to evaluate the photoresponse of a photodetector (find more details in the Supporting Information). Figure 3b shows the R values of the 2D $Ga_{0.84}In_{0.16}Se$ photodetectors for various illumination lights at V = 5 V. For example, R is 258.6 A/W for 500 nm illumination, which is 92 times and 20 times higher than those of mechanically exfoliated 2D GaSe (2.8 A/W illuminated at 254 nm) and InSe (12.3 A/W illuminated at 450 nm; Please find more comparison data in Table S1).[9,13] The D^* value is in the range of 2×10^{12} to 4×10^{12} Jones, which is comparable to that of currently used silicon photodetector[30] (10^{12} Jones). Figure S6 shows the $I-V$ curves of the 2D $Ga_{0.84}In_{0.16}Se$ photodetector illuminated at 650 nm with different light intensities. The I_{ph} is directly proportion to $P^{0.3}$ as shown in Figure 3d, illustrating that part of the photogenerated carriers recombine through trap states (defects and impurities). In Figure 3d, it is obvious that the R values decrease with increasing illumination light intensity, which is due to trap states in either in 2D $Ga_{0.84}In_{0.16}Se$ alloy nanosheets or at the interface between the 2D $Ga_{0.84}In_{0.16}Se$ alloy and SiO_2 substrate and is similar to the trend seen in 2D InSe photodetectors.[13] The EQE is 64000% at 500 nm illumination as seen in Figure S7, which is 47 times higher than that of 2D GaSe photodetector (1364% illuminated by 254 nm).[9] These results demonstrate that the 2D $Ga_{0.84}In_{0.16}Se$ photodetector has a broadband photoresponse ranging from 500 to 700 nm and shows high photoresponse performance.

The photoresponse stability and photoresponse speed are another two key parameters for photodetectors. As seen in Figure 4a, the 2D $Ga_{0.84}In_{0.16}Se$ photodetector shows almost the same current level for each on/off cycle for 0 days and 60 days of storage in air, demonstrating good reproducibility and long-time stability of the photoswitching response. After storage in air for 60 days, the 2D $Ga_{0.84}In_{0.16}Se$ photodetector shows a slightly lower dark current and photocurrent, which may be attributed to surface adsorption. Photoresponse speed values for the 2D $Ga_{0.84}In_{0.16}Se$ photodetectors can be extracted from an enlarged curve of one on/off cycle of illumination light as shown in Figure 4b. The 2D $Ga_{0.84}In_{0.16}Se$ photodetector shows a rapid response time of 30 and 43 ms for the rise and decay processes, respectively, which is comparable to those of 2D GaSe[9] and InSe[13] photodetectors.

In summary, we investigated the electronic and optoelectronic properties of 2D $Ga_{0.84}In_{0.16}Se$ alloy nanosheets for the first time. The 2D $Ga_{0.84}In_{0.16}Se$ nanosheets were obtained by mechanical exfoliation methods from bulk $Ga_{0.84}In_{0.16}Se$ alloy samples. The synthesized $Ga_{0.84}In_{0.16}Se$ alloy samples have good crystallinity and a direct optical bandgap of 1.83 eV. The 2D $Ga_{0.84}In_{0.16}Se$ FETs show p-type conduction behavior with a mobility of 0.8 $cm^2\ V^{-1}\ s^{-1}$ and current on/off ratio of 1×10^5, which are slightly higher than those of 2D GaSe. The 2D $Ga_{0.84}In_{0.16}Se$ photodetectors show high photoresponse performance over a broad visible-light range of 500 to 700 nm. The responsivity value is 258 A/W for the alloy photodetectors illuminated at 500 nm, which is 92 times and 20 times higher than those of 2D GaSe and InSe photodetectors, respectively. In addition, the photodetectors based on 2D $Ga_{0.84}In_{0.16}Se$ also exhibit good stability and rapid photoresponse speed. Our results demonstrate that the 2D $Ga_{1-x}In_xSe$ alloy has great potential for use in photodetection and sensor devices.

■ ASSOCIATED CONTENT

Supporting Information

The Supporting Information is available free of charge on the ACS Publications website at DOI: 10.1021/acsami.8b15317.

DOI: 10.1021/acsami.8b15317
ACS Appl. Mater. Interfaces 2018, 10, 43299−43304

Descriptions of the experiment, XPS, XRD, Raman, TGA, and optical bandgap of $Ga_{0.84}In_{0.16}Se$, AFM image, calculated equations for field-effect mobility, contact resistance, responsivity, detectivity and external quantum efficiency, *I*−*V* curves of $Ga_{0.84}In_{0.16}Se$ photodetectors illuminated by 650 nm light with various intensities and the EQE illuminated by various lights (PDF)

AUTHOR INFORMATION

Corresponding Authors

*Email: wfeng@nefu.edu.cn.
*Email: hupa@hit.edu.cn.

ORCID

Mingjin Dai: 0000-0001-6009-1715
Wei Feng: 0000-0001-6902-0024
PingAn Hu: 0000-0003-3499-2733

Author Contributions

[†]M.Y. and H.L. contributed equally to this work.

Notes

The authors declare no competing financial interest.

ACKNOWLEDGMENTS

This work is supported by the National Natural Science Foundation of China (NSFC, 51802038 and 61505033), the China Postdoctoral Science Foundation funded project (2018M630329), the Fundamental Research Funds for the Central Universities (2572018BC14).

REFERENCES

(1) Novoselov, K. S.; Geim, A. K.; Morozov, S. V.; Jiang, D.; Zhang, Y.; Dubonos, S. V.; Grigorieva, I. V.; Firsov, A. A. Electric Field Effect in Atomically Thin Carbon Films. *Science* **2004**, *306*, 666−669.

(2) Wang, L.; Wu, B.; Chen, J.; Liu, H.; Hu, P.; Liu, Y. Monolayer Hexagonal Boron Nitride Films with Large Domain Size and Clean Interface for Enhancing the Mobility of Graphene-Based Field-Effect Transistors. *Adv. Mater.* **2014**, *26*, 1559−1564.

(3) Pawbake, A. S.; Pawar, M. S.; Jadkar, S. R.; Late, D. J. Large Area Chemical Vapor Deposition of Monolayer Transition Metal Dichalcogenides and Their Temperature Dependent Raman Spectroscopy Studies. *Nanoscale* **2016**, *8*, 3008−3018.

(4) Li, L.; Yu, Y.; Ye, G. J.; Ge, Q.; Ou, X.; Wu, H.; Feng, D.; Chen, X. H.; Zhang, Y. Black Phosphorus Field-Effect Transistors. *Nat. Nanotechnol.* **2014**, *9*, 372−377.

(5) Yao, J.; Zheng, Z.; Yang, G. All-Layered 2D Optoelectronics: A High-Performance UV−vis−NIR Broadband SnSe Photodetector with Bi_2Te_3 Topological Insulator Electrodes. *Adv. Funct. Mater.* **2017**, *27*, 1701823.

(6) Yao, J.; Yang, G. Flexible and High-Performance All-2D Photodetector for Wearable Devices. *Small* **2018**, *14*, 1704524.

(7) Joshi, P. D.; Joag, D. S.; Rout, C. S.; Late, D. J. Photosensitive Field Emission Study of SnS_2 Nanosheets. *J. Vac. Sci. Technol., B: Nanotechnol. Microelectron.: Mater., Process., Meas., Phenom.* **2015**, *33*, 03C106.

(8) Late, D. J.; Liu, B.; Luo, J.; Yan, A.; Matte, H.; Grayson, M.; Rao, C.; Dravid, V. P. GaS and GaSe Ultrathin Layer Transistors. *Adv. Mater.* **2012**, *24*, 3549−3554.

(9) Hu, P.; Wen, Z.; Wang, L.; Tan, P.; Xiao, K. Synthesis of Few-Layer GaSe Nanosheets for High Performance Photodetectors. *ACS Nano* **2012**, *6*, 5988−5994.

(10) Late, D. J.; Liu, B.; Matte, H. S. S. R.; Rao, C. N. R.; Dravid, V. P. Rapid Characterization of Ultrathin Layers of Chalcogenides on SiO_2/Si Substrates. *Adv. Funct. Mater.* **2012**, *22*, 1894−1905.

(11) Shenoy, U. S.; Gupta, U.; Narang, D. S.; Late, D. J.; Waghmare, U. V.; Rao, C. N. R. Electronic Structure and Properties of Layered Gallium Telluride. *Chem. Phys. Lett.* **2016**, *651*, 148−154.

(12) Feng, W.; Zheng, W.; Cao, W. W.; Hu, P. A. Back Gated Multilayer InSe Transistors with Enhanced Carrier Mobilities Via the Suppression of Carrier Scattering from a Dielectric Interface. *Adv. Mater.* **2014**, *26*, 6587−6593.

(13) Tamalampudi, S. R.; Lu, Y.-Y.; Kumar, U. R.; Sankar, R.; Liao, C.-D.; Moorthy, B. K.; Cheng, C.-H.; Chou, F. C.; Chen, Y.-T. High Performance and Bendable Few-Layered InSe Photodetectors with Broad Spectral Response. *Nano Lett.* **2014**, *14*, 2800−2806.

(14) Bandurin, D. A.; Tyurnina, A. V.; Yu, G. L.; Mishchenko, A.; Zólyomi, V.; Morozov, S. V.; Kumar, R. K.; Gorbachev, R. V.; Kudrynskyi, Z. R.; Pezzini, S.; Kovalyuk, Z. D.; Zeitler, U.; Novoselov, K. S.; Patanè, A.; Eaves, L.; Grigorieva, I. V.; Fal'ko, V. I.; Geim, A. K.; Cao, Y. High Electron Mobility, Quantum Hall Effect and Anomalous Optical Response in Atomically Thin InSe. *Nat. Nanotechnol.* **2017**, *12*, 223−227.

(15) Pawbake, A. S.; Waykar, R. G.; Late, D. J.; Jadkar, S. R. Highly Transparent Wafer-Scale Synthesis of Crystalline WS_2 Nanoparticle Thin Film for Photodetector and Humidity-Sensing Applications. *ACS Appl. Mater. Interfaces* **2016**, *8*, 3359−3365.

(16) Pawbake, A. S.; Sandesh, R. J.; Dattatray, J. L. High Performance Humidity Sensor and Photodetector Based on SnSe Nanorods. *Mater. Res. Express* **2016**, *3*, 105038.

(17) Yao, J.; Shao, J.; Wang, Y.; Zhao, Z.; Yang, G. Ultra-Broadband and High Response of the Bi_2Te_3−Si Heterojunction and Its Application as a Photodetector at Room Temperature in Harsh Working Environments. *Nanoscale* **2015**, *7*, 12535−12541.

(18) Koppens, F. H. L.; Mueller, T.; Avouris, P.; Ferrari, A. C.; Vitiello, M. S.; Polini, M. Photodetectors Based on Graphene, Other Two-Dimensional Materials and Hybrid Systems. *Nat. Nanotechnol.* **2014**, *9*, 780−793.

(19) Mak, K. F.; Shan, J. Photonics and Optoelectronics of 2D Semiconductor Transition Metal Dichalcogenides. *Nat. Photonics* **2016**, *10*, 216−226.

(20) Late, D. J.; Shaikh, P. A.; Khare, R.; Kashid, R. V.; Chaudhary, M.; More, M. A.; Ogale, S. B. Pulsed Laser-Deposited MoS_2 Thin Films on W and Si: Field Emission and Photoresponse Studies. *ACS Appl. Mater. Interfaces* **2014**, *6*, 15881−15888.

(21) Zhou, X.; Cheng, J.; Zhou, Y.; Cao, T.; Hong, H.; Liao, Z.; Wu, S.; Peng, H.; Liu, K.; Yu, D. Strong Second-Harmonic Generation in Atomic Layered GaSe. *J. Am. Chem. Soc.* **2015**, *137*, 7994−7997.

(22) Bailey, R. E.; Nie, S. Alloyed Semiconductor Quantum Dots: Tuning the Optical Properties without Changing the Particle Size. *J. Am. Chem. Soc.* **2003**, *125*, 7100−7106.

(23) Liu, Y.; Zapien, J. A.; Shan, Y. Y.; Geng, C.-Y.; Lee, C. S.; Lee, S.-T. Wavelength-Controlled Lasing in $Zn_xCd_{1-X}S$ Single-Crystal Nanoribbons. *Adv. Mater.* **2005**, *17*, 1372−1377.

(24) Li, H.; Duan, X.; Wu, X.; Zhuang, X.; Zhou, H.; Zhang, Q.; Zhu, X.; Hu, W.; Ren, P.; Guo, P.; Ma, L.; Fan, X.; Wang, X.; Xu, J.; Pan, A.; Duan, X. Growth of Alloy $Mos_{2x}Se_{2(1-X)}$ Nanosheets with Fully Tunable Chemical Compositions and Optical Properties. *J. Am. Chem. Soc.* **2014**, *136*, 3756−3759.

(25) Duan, X.; Wang, C.; Fan, Z.; Hao, G.; Kou, L.; Halim, U.; Li, H.; Wu, X.; Wang, Y.; Jiang, J.; Pan, A.; Huang, Y.; Yu, R.; Duan, X. Synthesis of $Ws_{2x}Se_{2-2x}$ Alloy Nanosheets with Composition-Tunable Electronic Properties. *Nano Lett.* **2016**, *16*, 264−269.

(26) Yao, J.; Zheng, Z.; Yang, G. Promoting the Performance of Layered-Material Photodetectors by Alloy Engineering. *ACS Appl. Mater. Interfaces* **2016**, *8*, 12915−12924.

(27) Zheng, Z.; Yao, J.; Yang, G. Centimeter-Scale Deposition of $Mo_{0.5}W_{0.5}Se_2$ Alloy Film for High-Performance Photodetectors on Versatile Substrates. *ACS Appl. Mater. Interfaces* **2017**, *9*, 14920−14928.

(28) Antonangeli, F.; Piacentini, M.; Balzarotti, A.; Girlanda, R.; Grasso, V.; Doni, E. Electronic Properties of the III-VI Layer Compounds GaS, GaSe and InSe II: Photoemission. *Nuov. Cim. B* **1979**, *51*, 181.

(29) Zhou, Y.; Deng, B.; Zhou, Y.; Ren, X.; Yin, J.; Jin, C.; Liu, Z.; Peng, H. Low-Temperature Growth of Two-Dimensional Layered Chalcogenide Crystals on Liquid. *Nano Lett.* **2016**, *16*, 2103−2107.

DOI: 10.1021/acsami.8b15317
ACS Appl. Mater. Interfaces 2018, 10, 43299−43304

(30) Monroy, E.; Omnès, F.; Calle, F. Wide-Bandgap Semiconductor Ultraviolet Photodetectors. *Semicond. Sci. Technol.* **2003**, *18*, R33−R55.

DOI: 10.1021/acsami.8b15317
ACS Appl. Mater. Interfaces 2018, 10, 43299−43304